Presented at the 33rd JANNAF Combustion Subcommittee Meeting, Monterey, California, November, 1996.

The Thermal Decomposition Behavior of Ammonium Perchlorate and of an Ammonium-Perchlorate-Based Composite Propellant‡

Richard Behrens and Leanna Minier
Combustion Research Facility
Sandia National Laboratories
Livermore, CA 94551

ABSTRACT

The thermal decomposition of ammonium perchlorate (AP) and ammonium-perchlorate-based composite propellants are studied using the simultaneous thermogravimetric modulated beam mass spectrometry (STMBMS) technique. The main objective of the present work is to evaluate whether the STMBMS can provide new data on these materials that will have sufficient detail on the reaction mechanisms and associated reaction kinetics to permit creation of a detailed model of the thermal decomposition process. Such a model is a necessary ingredient to engineering models of ignition and "slow-cookoff" for these AP-based composite propellants.

Our results show that the decomposition of pure AP is controlled by two processes. One occurs at lower temperatures (240°C to 270°C), produces mainly H_2O, O_2, Cl_2, N_2O and HCl, and is shown to occur in the solid phase within the AP particles. 200μ diameter AP particles undergo 25% decomposition in the solid phase, whereas 20μ diameter AP particles undergo only 13% decomposition. The second process is dissociative sublimation of AP to $NH_3 + HClO_4$ followed by the decomposition of, and reaction between, these two products in the gas phase. The dissociative sublimation process occurs over the entire temperature range of AP decomposition, but only becomes dominant at temperatures above those for the solid-phase decomposition.

The results on the thermal decomposition of the AP-based composite propellant show several different features. First, the features of the two processes associated with the decomposition of the pure AP are still evident in the decomposition of the propellant. However, the oxidative products that evolve from the AP, such as O_2, Cl_2 and $HClO_4$, react to various extents with the plasticizer and binder in the propellant. The evolution rates of the gaseous products from the propellant sample, formed from the decomposition of AP within the propellant, are reduced compared to their evolution rates from pure AP. This reduced rate of evolution may be due initially to diffusion-limited flow of gas out of the sample, and at later stages, due to reduced flow through channels created by decomposition of the AP and binder. The reaction of the binder with $HClO_4$ occurs in a two-step sequence. First, most of the hydrogen is removed from the binder, then the remaining carbonaceous residue reacts with the oxidizers formed in the dissociative-sublimation/gas-phase reactions of AP to form CO and CO_2.

The results show that the STMBMS technique can be used to provide very detailed quantitative data on the decomposition of both pure AP and AP-based composite propellants. It appears that data of sufficient detail can be obtained that will allow a detailed engineering model of the thermal decomposition process to be created. Such a model will permit prediction of: the extent of decomposition of AP, plasticizer and binder; the identities and quantities of the gaseous reaction products; and the porosity and flow characteristics of the propellant as a function of time and temperature. Inclusion of these data in a 3D thermochemical code should allow the state of an AP-based composite propellant grain to be predicted when subjected to a thermal event, such as a fire.

INTRODUCTION

Ammonium-perchlorate-based composite propellants are used extensively in both small tactical rocket motors and large strategic rocket systems. The design of these systems is based on numerous and extensive studies conducted over the past four decades on the individual propellant ingredients[1] and their combustion in propellant formulations.[2,3] This knowledge has been successfully applied to design numerous AP-based composite propellant systems, such as the large solid rocket motors used on the space shuttle launch system. However, given this extensive base of knowledge, there are still outstanding questions that arise with regard to these propellants in the areas of response to abnormal environments (as characterized by fire, impact and/or shock) and of long-term aging effects on performance and safety. These issues are important to defense-based rocket motors that are both more likely to encounter abnormal environments, and are also presently starting to exceed the expectancy of their designed life due to the diminished rate of procurement of new replacement systems.

*Approved for public release; distribution is unlimited.

‡ Work supported by a Memorandum of Understanding between the U.S. Department of Energy and the Office of Munitions and by the U.S. Department of Energy under contract DE-AC04-94AL85000.

DISCLAIMER

In this paper, we present the results of initial experiments aimed at addressing the issue of the response of AP-based composite propellants in abnormal environments, specifically, the "slow cookoff" environment associated with fires. In a "slow cookoff" situation, heat flows slowly into the rocket motor, causing slow thermal decomposition of the individual ingredients to occur, followed by reactions between the ingredients of the propellant formulation. The heat generated by these reactions builds within the rocket motor, causing a reversal of the temperature gradient within the motor, and eventually leading to ignition deep within the propellant grain in the rocket motor. The resulting event after ignition may be a deflagration, an explosion, or possibly a detonation. The type of event that occurs will be determined by the state of the degraded material at the time of ignition. Possible changes that may be envisioned to occur in an AP-based composite propellant, consisting of primarily AP, aluminum powder and a hydroxy-terminated polybutadiene (HTPB) binder, include: 1) the formation of a multiphase porous media consisting of gaseous decomposition products (that may still contain significant potential to release heat in subsequent reactions) intermixed with condensed-phase reactants and products; 2) changes in the mechanical properties of the propellant due to reactions of the plasticizer and HTPB binder with decomposition products from the AP oxidizer; and 3) oxidation of the aluminum by the reaction with the decomposition products from AP.

The goal of our work on AP-based composite propellants is to determine the state of the propellant grain immediately prior to ignition. To accomplish this goal, we conduct thermal decomposition experiments using a simultaneous thermogravimetric modulated beam mass spectrometer (STMBMS) to study the thermal decomposition of both propellants and individual ingredients in the propellant formulation. In light of the extensive thermal decomposition work already done on AP and AP-based propellants, as summarize by Jacobs[1] and Kishore,[2] one may wonder what new information may still be obtained. In reviewing the literature, we have observed that indeed there have been extensive studies utilizing techniques such as: 1) conventional thermal analysis tools (i.e., evolved gas pressure, thermogravimetric analysis (TGA), differential thermal analysis (DTA) and differential scanning calorimetry (DSC)) to probe the weight loss and heat flow due to the chemical reactions; 2) mass spectrometric measurements to identify the products of reactions of individual ingredients; 3) optical observations of decomposing AP and quenched burning propellants; and 4) gas-phase measurements of the reaction kinetics of ammonia (NH_3) and perchloric acid ($HClO_4$), which arise from the dissociative sublimation of AP. However, there is little information on how the reaction chemistry of the ingredients may change when they are brought together in a propellant formulation and there are no chemical reaction kinetics data or models that can be used to predict the state of a propellant prior to ignition in a "slow cookoff" situation. Furthermore, even for AP, there is still not a clear picture of the reaction chemistry and physical processes that control its thermal decomposition, as evidenced by the review articles.[1,2]

In this paper we address three specific issues: 1) the thermal decomposition processes in AP; 2) whether our STMBMS technique is able to resolve mass spectra generated by the several constituents of an AP-based composite propellant formulation along with their decomposition products as the propellant is heated; and 3) what changes may occur in the decomposition processes of the individual ingredients due to their inclusion as part of a propellant formulation. Thus, this is our initial effort to determine whether STMBMS measurements of AP-based composite propellants will be able to provide sufficiently detailed chemical kinetics data to allow a detailed model of "slow cookoff" for these materials to be developed.

Based on the facts, that AP does not melt prior to decomposition, and that the decomposition of AP occurs in two separate temperature regimes, each producing different sets of gaseous products, as first observed by Dodé,[4,5] and subsequently by other investigators, Jacobs and Russell-Jones[6] formulated a unified mechanism for the decomposition of AP as summarized in R1.

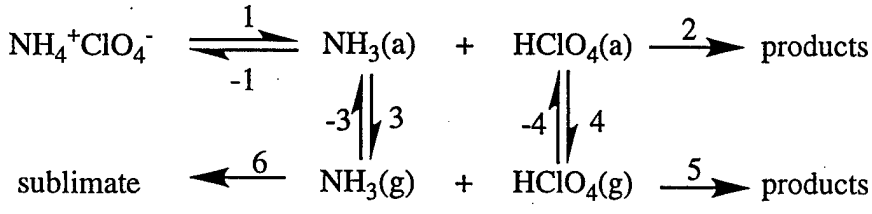

(R1)

In this model the AP undergoes a proton transfer to form ammonia and perchloric acid absorbed on the surface of the solid AP (step 1). The absorbates are in an equilibrium with gaseous NH_3(g) and $HClO_4$(g) (steps 3 and 4). The absorbates, NH_3(a) and $HClO_4$(a), react on the surface of the AP particles (step 2) to form the set of products observed in the lower temperature decomposition, Cl_2, N_2O, O_2 and H_2O. This lower temperature channel accounts for 30% of the decomposition of AP. The decomposition of AP is observed to stop at this point unless the sample is raised to higher temperatures. In the higher temperature channel the NH_3 and $HClO_4$ react in the gas phase to form

the final products, Cl_2, NO, O_2, and H_2O (step 5). Note that the higher temperature channel is observed to form NO rather than N_2O as observed in the lower temperature channel.

The controversial part of the mechanism proposed by Jacobs and Russell-Jones and presented in the review articles[1,2] is the low temperature mechanism and the reason for it stopping at 30% decomposition of the sample. In an extensive series of experiments, Bircumshaw and Newman[7,8] first discovered the low-temperature decomposition behavior of AP between 215°C and 275°C, in which the reaction stops after 30% of the sample decomposes. Through extensive experiments, in which the rate of gas pressure rise was measured as a function of sample size, particle size, inert gas overpressure, along with optical observations of the partially decomposed AP crystals, they conclude that the low-temperature decomposition begins by forming nucleating centers at defects on the surface of the AP particles and that the nuclei grow toward the center of the particle by forming channels that extend from the initial nucleating site. They speculate that this growth is due to an electron-transfer mechanism converting $NH_4^+ClO_4^-$ to $NH_4 + ClO_4$, followed by dissociation of NH_4 to $NH_3 + H$ and the transfer of charge between ClO_4 and other ClO_4^- anions within the lattice until a free ClO_4 reaches the surface of the particle where it undergoes decomposition to gaseous products. They proposed that the reaction terminates at 30% decomposition due to the disorder created in the distribution of ClO_4^- anions in the lattice, causing the electron-transfer process to cease. There was no direct evidence to support the electron transfer process. Mass spectrometric measurements of the decomposition of AP in a high vacuum environment[9] also yielded the first set of decomposition products, Cl_2, N_2O, O_2 and H_2O, indicating again that the reaction occurs in the solid phase, since gas-phase reactions between sublimating NH_3 and $HClO_4$ are essentially eliminated.

New insight into the decomposition processes of AP was developed by Kraeutle[10] through his hot-stage optical microscopy and SEM observations of the decomposition of AP crystals in the orthorhombic (< 240 °C) and cubic (> 240 °C) phases at temperatures between 200 °C and 300 °C. He found that AP starts to decompose at 225°C, forming pits on the surface of the crystals due to sublimation of the AP. He also observed the formation of blisters beneath the AP crystal surface that grow and eventually burst and attributed this process to the solid phase decomposition process. Upon heating to higher temperatures, he observed the transformation from the orthorhombic to the cubic phase, followed by nucleation of reaction sites deep within the crystal, the fast growth of the nuclei, the development of huge blisters, and the generation of cavities that can be 100-1000 times as large as the pores obtained in the orthorhombic phase. This decomposition also stops after 30% of the sample is consumed. Upon cooling the sample through the cubic --> orthorhombic phase transition, he observed severe damage to the crystals in the form of numerous cracks. This work provides the basis for an alternative model to R1 for the solid-phase decomposition of AP, in which nucleation sites are created within the crystals that may grow by the same dissociative sublimation/gas-phase reactions, as observed to occur between the NH_3 and $HClO_4$ evolved from the surface of the particles. However, due to containment of the gaseous products within crystals, the pressure of the contained gas is very high, driving the reaction of $NH_3 + HClO_4$ toward final products at lower temperatures.

The implications of this decomposition behavior of AP relative to the response of an AP-based composite propellant may be quite important. For example, ignition of a bed of thermally degraded propellant that consists of a porous solid, filled with reactive gases, can lead to an explosion as the gas-phase flame moves rapidly through the bed, causing the remaining solid propellant to ignite immediately. In addition, the formation of gaseous pockets within the propellant increases the density of potential "hot spots" within the material, thus, increasing the possibility of a transition to detonation once it is ignited.

In this paper, we present the results of our STMBMS thermal decomposition experiments on AP and an AP-based composite propellant. The results are discussed in terms of the previous studies on AP and the effects of other propellant ingredients on the decomposition process.

EXPERIMENTAL

INSTRUMENT DESCRIPTION.

The STMBMS apparatus and basic data analysis procedure have been described previously.[11-13] This instrument allows the concentration and rate of formation of each gas-phase species in a reaction cell to be measured as a function of time by correlating the ion signals at different m/z values measured with a mass spectrometer with the force measured by a microbalance at any instant. In the experimental procedure, a small sample (~10 mg) is placed in an alumina reaction cell that is then mounted on a thermocouple probe that is seated in a microbalance. The reaction cell is enclosed in a high vacuum environment ($< 10^{-6}$ torr) and is radiatively heated by a bifilar-wound tungsten wire on an alumina tube. The molecules from the gaseous mixture in the reaction cell exit through a small diameter orifice (25μ and 230μ in these experiments, orifice length is 25μ) in the cap of the reaction cell, traverse

two beam-defining orifices before entering the electron-bombardment ionizer of the mass spectrometer where the ions are created by collisions of 20 eV electrons with the different molecules in the gas flow. A relatively low electron energy of 20 eV (compared to 70 eV used on normal mass spectrometry measurements) is used to reduce the extent of fragmentation of the higher molecular weight ions and thus, limit their contribution to ion signals measured at lower m/z values that are associated with the thermal decomposition products. The background pressures in the vacuum chambers are sufficiently low to eliminate significant scattering between molecules from the reaction cell and background molecules in the vacuum chambers. The different m/z-value ions are selected with a quadrupole mass filter and counted with an ion counter. The gas flow is modulated with a chopping wheel and only the modulated ion signal is recorded. The containment time of gas in the reaction cell is a function of the orifice area, the free volume within the reaction cell, and the characteristics of the flow of gas through the orifice. The reaction cell used in the experiments has been described previously.[14] The cap in the reaction cell is now sealed using vacuum grease and an o-ring between the taper plug and the gold-foil pinhole orifice. The time constant for exhausting gas from the cell is small compared to the duration of the experiments (>~1000 sec). Note that the containment time of gas within the reaction cell is short once the gas molecules are in the free volume of the cell, but it may be much longer if the gas is trapped in the condensed-phase of the material within the cell. The pressure of the gaseous products within the reaction cell depend on the degree of confinement of the gaseous products. The pressures range from less that 1 torr for experiments with the larger diameter orifices (230μ) and lower confinement, to approximately 15 torr for experiments with smaller diameter orifices (25μ), and higher confinement.

ANALYSIS PROCEDURES

The thermal decomposition data on AP has been analyzed using the general procedure described previously.[13] For the decomposition of pure AP, the ion signals measured with the mass spectrometer are corrected for fragmentation of the AP sublimation products, NH_3 and $HClO_4$, by measuring the mass spectrum of these two products as they sublime from AP between 160 °C and 210°C. Specific ion signals, corrected for the contribution from fragmentation of NH_3 and $HClO_4$ in the mass spectrometer, are: NH_2(m/z=16), HCl(m/z=36), ClO_2(m/z=67), and ClO_3(m/z=83). Contributions to ion signals observed at other m/z values during the thermal decomposition of AP from NH_3 and $HClO_4$ were either small enough to be excluded from the present analysis or nonexistent.

The thermal decomposition data obtained from the AP-based propellants were quantified by using the sensitivity factors determined in a corresponding experiment using only AP in a reaction cell with the same orifice diameter. Products formed only from the propellant, and not AP, were either quantified by using a sensitivity factor of a similar type of gas, measured in the AP experiment, and estimating the relative ion formation probabilities (RIFP) for each species in the pair to determine the sensitivity factor of the new species, or not quantified in the present analysis.

MATERIALS

The AP-based propellant and its individual constituents that are used in this study were obtained from Ms. L. Dimeranon (NAWC, China Lake). Table I lists the constituents used in the propellant. All materials were used as received. Both the 20μ and 200μ average particle diameter lots of AP contained approximately 0.1% of tricalcium phosphate (TCP) stabilizer. Details of the particle characteristics (e.g., shape, surface area and particle size distribution) will be presented in a future paper that contains more detailed measurements of the decomposition process.

Table I. Description of the AP-based propellant formulation.

Component	*~ Weight Percent (%)*	*Structure*
AP (200μ)	50	NH_4ClO_4
AP (20μ)	20	NH_4ClO_4
Aluminum powder	20	Al (spheres)
Butadiene binder (HTPB is prepolymer)	7	$\{-CH_2-CH=CH-CH_2-\}_n$ *(some H replaced with hydroxy group)
DOS (plasticizer) {bis-2-ethylhexyl sebacate}	2	$-[-(CH_2)_4CO-CH_2CH-(C_2H_5)(CH_2)_3CH_3]_2$
other additives	~1	curing and bonding agents, antioxidants

RESULTS

The results presented in this paper are representative of our first efforts to utilize STMBMS to study an AP-based composite propellant. Therefore, they are not comprehensive in nature and basically represent an evaluation of whether or not STMBMS can be used to derive new data that can be used to develop new models of "cookoff" behavior. We present results from experiments used to test and evaluate the STMBMS method. For example, our experiments on AP evaluate the effects of the degree of containment of thermal decomposition products and the effect of particle diameter on the decomposition process, but not the effect of heating rate. In our experiments with propellant, we evaluate the effects of confinement of the gaseous products, but not the effects of sample geometry, which may influence the rate of release of gaseous products due to transport processes within the decomposing propellant. In the data that we present, we have extended the analysis of the STMBMS data to its furthest possible extent. This analysis involves: 1) assessing the mass spectral data to resolve the identities of the thermal decomposition products for AP and to resolve both the evaporating reactants and their thermal decomposition products for the propellant; 2) correction of the mass spectral data for fragmentation of reactants and products by electron-bombardment-induced fragmentation in the mass spectrometer; 3) smoothing the mass spectral data, representative of evaporating reactant and thermal decomposition products, for use in the quantification procedure; and 4) quantification of the results by correlating the mass spectral signals for the evaporating reactants and products with the rate-of-force-change data measured with the microbalance, to provide the rate of formation of the gaseous products and their pressures within the reaction cell as a function of time. We believe that this represents a rigorous evaluation of the STMBMS technique for use in studying AP-based composite propellants.

THERMAL DECOMPOSITION OF AMMONIUM PERCHLORATE.

The results of four experiments with AP are presented. The sample size, particle size and other parameters used in each experiment are listed in Table II.

Table II. Experimental parameters.[1]

Experiment	*I*	*II*	*III*	*IV*	*V*	*VI*
material[2]	AP	AP	AP	AP	propellant	propellant
particle diameter (μ)	200	200	20	200	20/200	20/200
sample size (mg)	10.2	10.2	10.4	10.4	10.5	12.4
orifice size (μ)	230	25	230	230	25	230

[1]Heating ramp rate is 1°C/minute from 100° to ~500°C for all experiments except IV, which is a ramp to 280°C and then cycle between 280°C and 200°C.
[2] AP is from lots used in propellant formulation. The propellant is a composite of (AP/Al/HTPB).

Effects of containment of gaseous products. Experiments were conducted with 200μ diameter AP particles, using orifice diameters ranging from 230μ down to 5μ. The results from experiments with the 230μ and 25μ orifices are presented here and represent the same trend as observed in experiments with orifice diameters down to 5μ. The pressure of the major decomposition products formed in Experiments I and II, for orifice diameters of 230μ and 25μ respectively, as a function of sample temperature are shown in Fig. 1. Several interesting features can be observed in this figure. First, there is a common set of peaks that occur between 240°C and 275°C and the temporal behavior of the products in this region is similar. Second, there is a another set of peaks, observed in Exp. II with the 25μ orifice, appearing between 280°C and 375°C, which are absent in Exp. I with the 230μ orifice. Third, the maximum gas pressure in the reaction cell in Exp. I is 0.3 torr and in Exp. II is 14 torr, a trend that is expected for these two different size orifices.

The decomposition behavior of 200μ AP in Exp. I (230μ) is illustrated by the gas formation rates of the decomposition products shown in Fig. 2. The gas formation rates (GFR) shown in Figure 2 (and all subsequent figures) are in units of 10^{-9} moles/sec so that direct comparison can be made between the rates of gas formation of the different products. Panels A through E in Fig. 2 shows the GFR between 200°C and 400°C and allows direct comparison to the subsequent AP and propellant data. From the GFR data shown Fig. 2, Panels A and B, two groups of major decomposition products are formed during the decomposition of AP under low-confinement conditions: 1) H_2O, O_2, N_2O, Cl_2 and HCl between 240°C and 270°C; and 2) NH_3 and $HClO_4$ from 200°C up to 315°C when the sample is depleted. The rate of gas formation of NH_3 and $HClO_4$ are almost equal during the decomposition, which is consistent with dissociative sublimation of AP with little reaction between the NH_3 and $HClO_4$ in the gas phase. Note that there appears to be H_2O evolving (Panel A) that has the same temporal behavior

of NH_3 and $HClO_4$. This may be due to water formed in the process between 240°C and 270°C that evolves as the rest of the sample evaporates, or it may be due to fragmentation of $HClO_4$ in the mass spectrometer, which has not been corrected due to experimental difficulties. More details of the products with lower GFRs are shown in Panels C and D. It is interesting to note that smaller amounts of NO and NO_2 are also formed during the decomposition, in addition to the previously reported N_2O. The N_2 GFR also increases in the same time period associated with the dissociative sublimation of AP (Panel D). It is highly unlikely that this N_2 is formed from NH_3 and $HClO_4$ in the mass spectrometer and it seems equally unlikely that it is formed in a gas-phase reaction in the reaction cell, since the low-pressure conditions do not favor driving the $NH_3 + HClO_4$ reaction toward final products. Thus, it suggests that the N_2 may actually evolve from nitrogen that was trapped in the AP during its preparation.

The gas formation rates of the chlorine oxides that are formed in the first steps of the thermal decomposition of $HClO_4$ and $NH_3 + HClO_4$ reactions are shown in Fig. 2, Panel E. The purpose of showing these data is to illustrate the ability of the STMBMS technique to detect the first stages of the gas-phase reactions. However, at the present stage of our experiments and analysis, the results only show the approximate gas formation rates of these products with respect to the major products, NH_3 and $HClO_4$. They do not accurately give the relative GFRs between the various chlorine oxides. This is due to incomplete correction of the mass spectral data for fragmentation of the $HClO_4$ and the use of approximate relative-ion-formation-probabilities (RIFPs) to relate the flux of the various chlorine oxides through the mass spectrometer to their ion signals. The ClO_2 and ClO_3 products are corrected for contributions from ion fragmentation, whereas the other products are not.

The gas formation rates of the products, formed in the low temperature channel in Exp. I, are shown in more detail in Fig. 2, Panels F through H. There is high degree of temporal correlation between the H_2O, O_2, N_2O, Cl_2, N_2 and NO GFRs, but there is a very significant lag in the HCl GFR with respect to the GFR of the other products(Panel G). (Note that the dip in the N_2O signal is due to noise in the data). The identity of the products formed in this low-temperature channel is indicative of the final products of the $NH_3 + HClO_4$ reaction and not the initial products, such as the chlorine oxides. Comparison of the products formed in the low-temperature channel with those formed from the $NH_3 + HClO_4$ sublimation/gas-phase reaction process, indicates that reaction conditions exist within the particles producing high gas densities that drive the $NH_3 + HClO_4$ reaction toward its final products. This behavior strongly supports a solid-phase decomposition process accounting for the low-temperature channel. The additional fact that HCl lags the other products suggests that it is, at least partially, due to changes in the particle morphology and increased porosity of the particles since HCl is a product of less complete reaction of $HClO_4$.

From these results it is apparent that two processes control the decomposition of AP: 1) solid-phase decomposition; and 2) dissociative sublimation of AP to $NH_3 + HClO_4$ followed by reaction of NH_3 with $HClO_4$.

The decomposition behavior of 200μ AP in Exp. II (25μ orifice) is illustrated by the gas formation rates of the decomposition products shown in Fig. 3. The main products of the decomposition are again illustrated by the GFRs shown in Panels A and B. The behavior of the GFRs of the products associated with the solid-phase decomposition channel is similar to Exp. I. In contrast, the behavior of the products associated with the dissociative sublimation channel are significantly different. First, the reaction continues to a higher temperature (385°C vs. 315°C for Exp. I) due to the reduced flow rate of the AP dissociative equilibrium products, NH_3 and $HClO_4$, out of the reaction cell, which is caused by the smaller orifice diameter. Second, due to the increased number gas-phase collisions, reactions of NH_3 and $HClO_4$ increase. The corresponding rate of flow of NH_3 and $HClO_4$ changes from being equal in Exp. I to the flow rate of $HClO_4$ out of the cell being approximately four times greater than NH_3 in Exp. II (Fig. 3, Panel B). Third, the GFRs of the reaction products of the dissociative sublimation channel (H_2O, HCl, O_2, N_2O and Cl_2) are about five times higher than the GFRs of NH_3 and $HClO_4$, indicating that there is a substantial amount of reaction in the gas phase in this experiment. Fourth, the ratio of the GFRs for HCl to Cl_2 is 7 to 10 for the dissociative-sublimation channel, whereas, it is 0.5 to 1 in the solid-phase channel. This behavior is consistent with less complete reactions occurring in the gas phase under the relatively low pressures in the reaction cell (see Fig. 1).

The results for the reaction products with lower GFRs are shown in Fig. 3, Panels C and D. The GFRs for Cl_2, N_2O, NO_2 and NO and N_2 in the solid-phase decomposition channel are approximately the same for Experiments I and II. The ratio of N_2O to Cl_2 may be slightly higher in Exp. II than Exp. I in the solid-phase decomposition. The products formed in the dissociative sublimation channel in addition to the major product listed above include N_2O, N_2, NO_2 and NO. The chlorine oxides formed in the dissociative sublimation channel are ClO_2 and ClO_3 shown in Fig. 3, Panel E. In this experiment, the ClO_3 GFR is greater than the ClO_2 GFR, which is opposite to the behavior observed in Exp. I.

The gas formation rates of the decomposition products formed in the solid-phase decomposition channel are shown in Fig. 3, Panels F through I. The GFRs of H_2O, O_2, N_2O, Cl_2, NO_2, N_2 and NO are all highly temporally

correlated, as they were in Exp. I. The GFRs are all about the same as the corresponding GFRs in Exp. I. One notable exception is the slightly lower GFR of Cl_2 in Exp. II. This difference may be real or may possibly be an artifact of the analysis of the data. Further experiments will clarify this point. The GFR of HCl also lags the other products in a manner similar to that observed in Exp. I. Again, this suggests that loss of gas confinement leads to the formation of HCl, a product of less complete reaction. Two products observed from the solid-phase decomposition channel in this experiment and not as obvious in Exp. I, due to their high sublimation rates, are NH_3 and $HClO_4$ (Panel F). The NH_3 is temporally correlated with the other major products formed in the solid-phase decomposition channel. It is formed in the same reaction process that accounts for the other products. However, the $HClO_4$ product evolution is delayed with respect to the major products. It may correlate with the delay observed in the HCl signal. One may speculate on the origin of the peak in the GFR of $HClO_4$ shown in Panel F. It may be due to a higher temperature from the release of heat in the solid phase decomposition causing the dissociation pressure AP to rise. Lack of a corresponding peak in the NH_3 GFR suggests that this may not be the correct explanation. Another possibility is that during the solid-phase decomposition within the particles, the surface that is at the gas bubble boundary, becomes depleted in NH_3. After the bubbles burst and the solid-phase reaction stops, perchloric acid sublimes from the $HClO_4$ enriched surface, until a normal AP surface is reached and the usual NH_3 + $HClO_4$ sublimation resumes. Further investigations may help clarify this point.

Both experiments on the effects of confinement on the decomposition of AP produce consistent results. The AP decomposes by two processes. One is decomposition in the solid phase in which approximately 25% of the sample decomposes in the solid phase. The other is dissociative sublimation of AP to NH_3 + $HClO_4$ with the subsequent gas-phase reactions of ammonia and perchloric acid.

Effects of thermal cycling. The extent of reversibility of the solid-phase decomposition process can be assessed by heating a new sample of AP and then ramping the sample through subsequent heating and cooling cycles to see whether the solid-phase decomposition occurs again on subsequent cycles. The results from Exp. III, in which 200μ diameter AP in a reaction cell with a 230μ diameter orifice is heated to 280°C and then cycled between 280°C and 200°C at 1°C/min. is shown in Figure 4. The data are plotted on a semilog plot to accentuate the behavior at low GFRs. The data in Panel A shows that, on the first heating cycle, the normal solid phase decomposition products are observed, H_2O, O_2, N_2O, Cl_2 and HCl. On the subsequent cooling and heating cycles these products stay at least two orders of magnitude below their peak values on the first thermal decomposition ramp. Each successive cycle generates less of the decomposition products. One interesting feature, present on the original mass spectral data, but lost in the quantification process, is a small peak on the GFRs of H_2O and Cl_2 occurring as the sample is cooled from 240°C and 220°C. This temperature range corresponds to the cubic --> orthorhombic phase transition and suggests that some of the final products from the solid-phase decomposition process are forced out of the lattice as it undergoes the phase transition.

The main process that occurs during the temperature cycling process (following the initial thermal cycle) is the dissociative sublimation of AP to NH_3 and $HClO_4$, as illustrated by the data in Fig. 4, Panel B. The GFRs of ammonia and perchloric acid clearly track the temperature ramp.

Effects of particle size. To evaluate the effect of particle size on the thermal decomposition of AP, experiments were conducted on AP powders having a 20μ mean particle diameter. The results of one of these experiments (Exp. IV), using a 230μ diameter orifice, is shown in Fig. 5. The data have the same general features as the corresponding experiment with 200μ diameter AP powder (Exp. I, Fig. 2). The same general features of the solid phase decomposition products (Panel A) and the dissociative sublimation of NH_3 and $HClO_4$ (Panel B) are observed between the two experiments. The relative ratios between the GFRs of the solid phase decomposition products are the same for both the major products, H_2O, O_2, N_2O, Cl_2 and HCl, as well as the minor products, N_2, NO_2 and NO. The NH_3 and $HClO_4$ are also both formed at approximately equal rates, as is expected under these low confinement conditions.

The major difference between the decomposition of 20μ and 200μ diameter AP is in the absolute value of the GFRs of the solid-phase decomposition products compared to the dissociative sublimation products. The GFRs of NH_3 and $HClO_4$ are about 30% higher for the 20μ diameter powder than the 200μ diameter powder. This is reasonable since the orifice is relatively large and the AP, NH_3 and $HClO_4$ are in a quasi-equilibrium. Thus, the smaller particle size sample, having a larger surface area, can supply the quasi-equilibrium process at a higher rate and accounts for the higher measured GFRs for NH_3 and $HClO_4$. In contrast, the GFRs for the solid phase decomposition products are about a factor of 2.5 lower for the 20μ diameter particles than for the 200μ diameter particles, as can be seen by comparing Panels A, C and D in Figures 2 and 5. The other major difference between the data from the two different size particles is in the shape of the GFR curves characterizing the solid-phase decomposition as shown in Panels E, F and G. The data for the 20μ AP appears more sharply peaked.

Integration of the GFRs for the products from the solid-phase decomposition channel shows that only 13% of the 20μ diameter AP decomposes in the solid-phase channel compared to ~25% of the sample for the 200μ diameter AP. This indicates that decomposition of AP in the solid phase has a significant dependence on the particle size.

THERMAL DECOMPOSITION OF AP-BASED PROPELLANT.

The ingredients of the propellant used in the experiments are listed in Table I. The propellant basically consists of AP, aluminum, hydroxy-terminated polybutadiene (HTPB), a plasticizer (DOS), and several other minor ingredients. Ion signals, associated with the various ingredients in the propellant as it is heated from 25°C to 500°C in a reaction cell with a 230μ diameter orifice, are shown in Fig. 6. First the more volatile products, the plasticizer and two additives, evolve between 50°C and 200°C, followed by the decomposition products associated with AP between 200°C and 315°C, and finally products from decomposition of the binder evolve between 380°C and 450°C. Clearly, these results show that the STMBMS can resolve the different reactants associated with the propellant.

The real issue is to determine how effective STMBMS will be for determining the reaction mechanisms and measuring the associated reaction kinetics and transport properties that control the thermal decomposition processes in a propellant. To address this issue, we conducted several experiments on the AP-based propellant, listed in Table II, under different degrees of confinement. We used orifice diameters ranging from 230μ down to 5μ. The results from experiments with 230μ and 25μ diameter orifices have been analyzed and are presented here. These experiments were carried out under the same conditions as used for the pure AP experiments described above.

Propellant decomposition under higher confinement (25μ orifice). Careful examination of the GFRs of the decomposition products from the propellant under higher confinement and comparison with the pure AP results provides significant insights into the thermal decomposition processes of the propellant. The gas formation rates of the decomposition products from the propellant sample used in Experiment V are shown in Fig. 7. Panel A shows the GFRs of the five most abundant products as the propellant is heated between 200°C and 400°C. Panel B shows the corresponding GFRs of NH_3 and $HClO_4$. Panels C and D show the GFRs of the thermal decomposition products formed at lower rates. Panel E shows the GFRs of CO and CO_2, two new products produced by reaction between the AP and the plasticizer and binder. (Note: The CO and CO_2 GFRs were determined by correcting the m/z=28 and m/z=44 mass spectral signals for N_2 and N_2O. This was done by using correlations between the N_2 (m/z=28) and N_2O (m/z=44) signals with Cl_2 in the solid-phase decomposition portion of the data and with $HClO_4$ in the sublimation portion of the data, based on correlations observed between these signals in the experiments with pure AP. Next, the sensitivity coefficients for CO and CO_2 were determined by optimizing the coefficients to achieve elemental mass balance for the non-aluminum portion of the propellant.)

Direct comparison of these data with the GFRs of the decomposition products from pure AP, taken under similar conditions (Exp. II, Fig. 3), show quite different results. Comparison of the solid-phase decomposition portion of the data, between 240°C and 275°C, for the propellant and pure AP show the following differences: 1) the maximum GFR for H_2O is four times higher in the pure AP than in the propellant; 2) the H_2O peak, as well as the peaks for the other products, are significantly broader in the propellant than in the pure AP; 3) the GFRs for O_2 and Cl_2 are 10 times higher in the pure AP than in the propellant; 4) the N_2O peak is ~4.5 times higher in the pure AP than it is in the propellant; and 5) HCl GFR has about the same maximum value in the pure AP and the propellant but it is significantly broader in the propellant. From these observations, we draw two conclusions. First, the O_2 and Cl_2 formed in the solid-phase decomposition of AP react with the plasticizer and/or the binder to form H_2O and HCl. Second, the transport of the products, formed in the solid-phase decomposition of AP, along with the products formed by reaction of AP with the plasticizer/binder, is inhibited due to the restricted flow of gases within the propellant formulation. As reaction of the propellant progresses, the propellant becomes more porous and the restriction of gas flow should decrease.

The differences observed in the dissociative-sublimation/gas-phase reaction channel between the pure AP and the propellant are even more dramatic than those observed for the solid-phase portion of the decomposition. Comparison of the behaviors of the GFRs of NH_3 and $HClO_4$ between the pure AP and the propellant (Panel B in Figs. 3 and 7) indicate that significant reaction between the perchloric acid and the binder occurs (the signal associated with DOS disappears in the same time frame as the solid-phase decomposition channel in Exp. V). In pure AP, the $HClO_4$ GFR is greater than the NH_3 GFR, and is determined by the gas-phase reactions in the reaction cell. In contrast, the $HClO_4$ signal in the propellant is zero until the sample reaches about 310°C, at which point its signal starts to rise in a manner similar to that observed in pure AP. The ammonia signal is approximately 5 times higher in the propellant than in the pure AP up to about 275°C. Between 275°C and 315°C it rises very rapidly becoming over 10 times larger in the propellant than in the pure AP. This behavior of the $HClO_4$ and the NH_3 GFRs indicates that the sublimation rate increases in an attempt to maintain the dissociative equilibrium between AP, NH_3 and $HClO_4$ as the perchloric acid reacts with the binder. Further evidence for perchloric acid reacting with

the binder is found between 275°C and 315°C in the high GFRs for H_2O and HCl in the propellant and very low GFRs for these two products in the pure AP.

The decomposition process in the propellant changes again at about 310°C. At this point there is a dramatic drop in the GFR of ammonia, a rise in the GFR of $HClO_4$ from its zero value, a drop in the H_2O and HCl signals, an abrupt increase in the GFR of O_2, and a rapid rise in the GFRs of CO and CO_2. This behavior indicates that the reaction of perchloric acid with the binder is ending, having removed most of the hydrogen from the binder in the form of H_2O and HCl products. The remaining AP then reacts in a manner similar to the pure AP, as indicated by the increase in the GFRs of H_2O, O_2, N_2O, HCl and Cl_2 above 315°C. However, as the AP dissociation product GFRs start to rise at 315°C there is also a rapid rise in the GFRs of CO and CO_2. The GFRs of CO and CO_2 are sharply peaked between 310°C and 330°C. Since the only carbon remaining in the system is the residue left after the reaction between the binder and the perchloric acid, the evolution of CO and CO_2 is due to the reaction between the remaining AP and the residual carbonaceous material left from the binder. After the CO and CO_2 GFRs drop, indicating complete reaction of the binder residue, the normal pure AP decomposition products resume their individual decomposition reaction until the sample is depleted at 340°C.

It is interesting to note that due to the changes in the reactions of the AP when in the presence of the other ingredients in the propellant, the reaction occurs in a significantly shorter period of time (100 minutes for the propellant and 140 minutes for the pure AP).

Propellant decomposition under lower confinement (230μ orifice). Careful examination of the GFRs of the decomposition products from the propellant under lower confinement conditions (Exp. VI, Figure 8) and comparison to the GFRs of the decomposition products from pure AP under similar conditions (Exp. I, Fig. 2), shows several features of the decomposition process in addition to those observed in the higher confinement case.

The decomposition products from the solid-phase decomposition channel are released from the sample more rapidly in the lower confinement experiment. The gas formation rates of the decomposition products from the solid-phase channel have higher maximum GFRs in the case of lower confinement of the propellant compared to the higher confinement case (Panel A in Figs. 7 and 8). The width of the peaks in the lower confinement case are not as broad as in the higher confinement case with the propellant. However, the maximum GFRs are less and the width of the peaks are broader for the solid-phase decomposition products in the propellant compared to those of the pure AP (Panel A, Figs 2 and 8). This result suggests that confinement of gas products in the vicinity of the propellant has a significant effect on the release rate of products from the propellant. It also indicates that the STMBMS technique can be used to obtain meaningful information on this process.

The other interesting feature that is observed in the lower confinement experiment with the propellant is the interaction between the perchloric acid and the binder. In the lower confinement case, the plasticizer evaporates before the AP decomposition reaction starts, so that reaction of the $HClO_4$ occurs with only the binder in this experiment. As can be seen from Panel B in Fig. 8, the GFR of $HClO_4$ is not zero as it was in the higher confinement case. However, it is below the GFR of NH_3 (for the pure AP the GFRs of these two products are equal), thus indicating that some of the $HClO_4$ reacts with the binder as it passes through the propellant. The increase in both the H_2O and the HCl GFRs above 275°C is also consistent with reaction between perchloric acid and the binder.

DISCUSSION

DECOMPOSITION OF PURE AP.

Our results on the decomposition of pure AP are consistent with most of the previous work on AP. We observe two separate processes that control its thermal decomposition. One occurs at a lower temperature, and in our experiments, with 200μ diameter AP, accounts for 25% of the decomposition products. The other occurs at higher temperatures and involves dissociative sublimation of AP.

Our results on decomposition in the lower temperature channel are consistent with previous studies that found that the process at low temperatures ceases when 30% of the sample has decomposed.[8] The products that evolve during the low-temperature process in our experiments are the same as those measured in previous work,[9] H_2O, O_2, N_2O and Cl_2. However, we also observe the evolution of HCl, NO_2 and NO at lower gas formation rates. Thus, other nitrogen oxides are formed in addition to those previously reported.

Our results show that the decomposition of AP in the low-temperature channel takes place in the solid phase within the individual AP particles. This conclusion is based on the identities of the products observed, the

invariance of the identities and GFRs of the products under different levels of confinement, and the decrease in the fraction of decomposition that occurs with smaller size AP particles. The main products formed in this channel are H_2O, O_2, N_2O and Cl_2. These products represent the final products expected from the decomposition of AP or the reaction between NH_3 and $HClO_4$, and thus, indicate that they were formed under high-pressure conditions. Under these conditions, the number density of the reactants is sufficiently high, so that enough reactive collisions occur, to produce final products. In our experiments, this high-pressure condition can only occur within the individual particles. This effect is further supported by the invariance of this process to the degree of confinement of gases in the reaction cell. One can also argue that the decrease in the GFRs and the total amount of decomposition products as the AP particle diameter decreases from 200μ down to 20μ also supports the argument for decomposition in the solid phase. The argument is as follows: For decomposition to occur within the solid particle, it probably occurs via a typical solid-phase decomposition process of nucleation and growth of reaction centers (bubbles in the case of gaseous products in AP). The growth of the reaction center may be a pressure-driven process in the case of AP. Therefore, once the solid can no longer support the gas pressure within the lattice, the gas is released and the reaction stops. The process will stop once the surface of the bubble in the AP crystal cracks and releases its gas from the particle. The cracking may be due to fracture near the surface of the particle or growth and coalescence of the bubbles within the particle to form channels for gas release. This model suggests that a certain portion of the particle near the surface will not have sufficient strength to support growth of a bubble at the nucleating center within a certain distance of the surface. For example, if one assumes that a surface layer 5μ thick cannot participate in the bubble growth process, then one predicts that only half as much AP is available for reaction in a 20μ diameter AP particle compared to a 200μ diameter AP particle. While this model of the decomposition process in the solid phase is speculative, it is consistent with our results. This model for decomposition is also consistent with the optical and SEM observations of AP decomposition by Kraeutle.[10] Kraeutle observed the nucleation and growth of bubbles deep within the AP crystals, followed by the eventual fracture of the bubbles and release of gases. The size of the features representing the approximate "particle diameters" of the remaining highly porous AP particles was between 3μ and 10μ.

The surface reaction mechanism (step 2 of Reaction R1), quoted extensively in the literature to account for decomposition in the low temperature channel, is not consistent with our results. First, the variation in the GFRs of the decomposition products in the low temperature channel when the particle diameter is changed from 200μ to 20μ, a factor of 100 increase in surface area, is not commensurate with such a large change in the surface area. In fact, the GFRs actually decrease with the increased surface area. Second, the decomposition is independent of the degree of containment of gaseous products. For the case of the two experiments investigating effects of the variation of confinement on the decomposition of AP, presented in this paper, the sublimation rate of AP should increase by approximately a factor of 100 when going from the experiment with the 25μ diameter orifice to the experiment with the 230μ orifice, due to the larger area of the orifice. One would expect this increased sublimation rate to have a very large effect on a decomposition process that occurs on a surface. We do not observe such an effect.

The surface decomposition mechanism was also proposed based on observations that NH_3 reduced the reaction rate[7,15] in the low temperature channel. From our results it is possible to see how this effect may occur. However, it is not in conflict with our conclusion that the decomposition process at the lower temperature occurs in the solid phase. In the AP decomposition experiment using the 25μ orifice (Exp. II, Fig. 3), we were able to observe the GFRs for NH_3 and $HClO_4$ produced during the solid-phase process (due to the reduced sublimation rate of NH_3 and $HClO_4$ in this experiment). Examination of the data in Fig. 3, Panel F shows that NH_3 evolves with the same temporal behavior as the major products of the decomposition in this channel. However, the temporal behavior of the $HClO_4$ is clearly shifted to longer times (10 min.) and higher temperatures (~ 10°C). This behavior most likely occurs due to excess perchloric acid being present on the surface of the AP at the end of the decomposition process in the low temperature channel. Since evolution of the $HClO_4$ product from the low temperature decomposition process starts to rise when the first major decomposition products appear, it suggests that as the gas bubbles formed in the solid AP rupture, they rapidly release the more volatile products, H_2O, O_2, N_2O, Cl_2, NH_3, and then slowly evolve the $HClO_4$ from the $HClO_4$-enriched surface. These results are consistent with reaction processes that occur in bubbles located within a solid particle. The growth of the bubbles is dependent on reaction processes occurring at the bubble's gas/surface interface. The addition of ammonia to the system may reduce the number of reactions that would occur after the more volatile products are released from the bubble, by reacting with the excess $HClO_4$ remaining on the surface. This may reform AP on the surface, due to reaction between NH_3 and $HClO_4$, and eliminate subsequent reactions in the enriched $HClO_4$ layer.

The other process that controls the decomposition of AP is the dissociative sublimation of AP to NH_3 and $HClO_4$ and the subsequent gas-phase reactions of these two products. As expected, results from our experiments with lower confinement show mostly NH_3 and $HClO_4$ evolving from the AP along with smaller quantities of ClO_2 and ClO_3, formed during the first steps of the decomposition reaction. In our experiment using higher confinement

of the gases, products associated with a more advanced stage of reaction toward the final equilibrium-type products are observed. Obtaining the detailed reaction kinetics of the $NH_3 + HClO_4$ is not one of the main objectives our current work on AP-based composite propellants. This chemical reaction has been studied extensively in previous work[1] and there are better techniques available, such as flow reactors or shock tubes, for obtaining further information on the $NH_3 + HClO_4$ reaction kinetics. To achieve the goals of our work, it is sufficient to identify and characterize the GFRs of the various products so that we can determine the amount of heat released from the chemical reactions and gain some insight into what products may be created that will react with the other propellant ingredients.

DECOMPOSITION OF AP-BASED PROPELLANT.

Decomposition of the AP-based composite propellant used in our experiments shows evidence of evaporation of the more volatile components, the two pure-AP decomposition processes, chemical reactions between the decomposition products from AP and the other propellant ingredients, and effects of restricted flow on the release of gaseous products from the propellant.

The gaseous products from the solid-phase decomposition of AP are also observed in the propellant. The decomposition process occurs in the same temperature range as in the pure AP. However, the ratios of the GFRs of the products released from the propellant are significantly different from pure AP. The GFRs for H_2O and HCl remain high while the GFRs for O_2 and Cl_2 drop significantly. This indicates that the O_2 and Cl_2 are reacting with the plasticizer and binder. In the case of our low-confinement experiment (Exp. VI), the plasticizer evaporates prior to the first decomposition of AP in the solid phase and the decomposition products from AP react only with the binder.

In addition, the release rate of products from the solid-phase decomposition channel of AP is reduced due to the restricted flow of gas out of the propellant sample. The flow rate of gaseous products out of the sample was reduced by increasing the overpressure of the gaseous products in the reaction cell. Being able to measure change in the gas release rates from the propellant, should allow experiments to be conducted in the future that will provide more quantitative data on the release process.

The evolution of decomposition products associated with the dissociative sublimation and subsequent gas-phase reactions of AP is significantly altered in the propellant. The general sequence of the reaction between the AP and the binder is summarized by the following three steps

$$NH_4ClO_4 \underset{}{\overset{1}{\rightleftharpoons}} NH_3(g) + HClO_4(g)$$

$$\left[C_{H_2}-C_{H}=C_{H}-C_{H_2}\right]_n + 1/2\,HClO_4 \xrightarrow{2} \left[C_4H_2\right]_n + 1/2\,HCl + 2H_2O$$

$$\left[C_4H_2\right]_n + 2HClO_4 \xrightarrow{3} \left[C_4H_2\right]_{n-1} + 2HCl + H_2O + CO + 3CO_2$$

The first step represents the dissociative sublimation of AP, the second step represents the reaction between $HClO_4$ and the binder to extract hydrogen and form HCl and H_2O, and the third step represents the reaction between perchloric acid (and possibly the oxidative products formed in gas-phase reactions of $HClO_4$) with the carbonaceous residue that remains after hydrogen has been extracted from the binder. The reaction sequence is strongly supported by the absence of perchloric acid evolution from the reaction cell up to about 315°C, the commensurate increase in the GFRs of H_2O and HCl between 275°C and 315°C, followed by a rapid increase in the GFRs of CO and CO_2.

The first apparent change in the decomposition of AP in the propellant (relative to that of pure AP) via the dissociative sublimation channel is the increased rate of sublimation of AP as evidenced by the shorter duration of the experiment. This increased reaction rate is due to the reaction between the perchloric acid and the binder, removing $HClO_4$ from the gas phase and thus driving the sublimation rate of AP higher as it tries to maintain the equilibrium with $NH_3(g)$ and $HClO_4(g)$. The increased GFR of NH_3 is a good measure of the sublimation rate of AP, since there are little oxidative species available to react with ammonia since they are primarily consumed by reaction with the binder. This conclusion is supported by very low GFRs of nitrogen oxides, while the $HClO_4$ is reacting with the binder to remove hydrogen (step 2). There is some possibility that NH_3 may react with the free radicals formed in the binder in an amination-type reaction.

The sequential removal of the majority of hydrogen from the binder (step 2), prior to oxidation of the remaining carbonaceous residue (step 3), will create free radicals in the remaining polymer, promoting cross-linking and the associated hardening of the material. This hardening process could have significant effects on the response of the propellant to impacts and shocks that may occur after the start of a "cookoff" event, since the ability of the binder to absorb and dissipate mechanical energy would be reduced.

The oxidation of the remaining carbonaceous binder is a relatively rapid process, once the majority of the hydrogen is removed from the binder. The increase in the GFRs of O_2, NO_2, and N_2O, at the same time that the CO and CO_2 evolve at their most rapid rates, suggests that any of these oxidizers, in addition to the $HClO_4$, may be involved in the oxidation of the remaining residue.

In the higher confinement experiment (Exp. V), the CO and CO_2 GFRs drop rapidly, indicating that most of the carbonaceous part of the binder has been oxidized, and the remaining AP resumes the formation of decomposition products in a manner similar to the that observed in the experiment with pure AP. In the experiment using lower confinement, there is incomplete reaction with the binder because the AP has sublimed or reacted before the reaction with the binder is complete, as indicated by the simultaneous decline in the NH_3, $HClO_4$, CO and CO_2 GFRs.

APPLICATION OF STMBMS MEASUREMENTS TO DEVELOPING DATA FOR MODELS OF "COOKOFF" OF AP-BASED COMPOSITE PROPELLANTS

The goal of this study has been to assess the utility of using the STMBMS technique to obtain data on the thermal decomposition of AP-based composite propellants that can be used to develop models that predict the time to ignition and the state of the propellant immediately prior to ignition in a "slow-cookoff" event. Given the number of ingredients in the propellant and the potential for generating very complex mass spectral data, our initial expectations for generating data that could be interpreted and used to generate a "slow-cookoff" model were not very high. However, the results we have obtained and our analysis of the data show that exceedingly detailed data can be obtained on many of the processes that are important to the thermal degradation of AP-based composite propellants.

In general, our results on the decomposition of AP and an AP-based propellant show features in the decomposition that have been observed by some of the other researchers in the past. However, most of the past investigations have either measured isolated aspects of the decomposition process (i.e., mass spectra of gases evolved during the decomposition of AP or heat release in a DSC measurement) or were based on physical or microscopic measurements (i.e., the optical microscopy and SEM work of Kraeutle). While these types of measurements are important for developing a qualitative understanding of the decomposition process, they are not able to provide the specific details of the thermal decomposition process nor the quantitative data required to construct a model that will predict the response of a propellant in a "slow-cookoff" event. The results that we have obtained with the STMBMS show that this technique is capable of obtaining the data required to construct a realistic model of ignition and a "slow-cookoff" event.

For pure AP, further experiments can be conducted that will completely characterize the identity and rates of formation of all the gaseous products as a function of temperature, heating rate and particle size. For the solid-phase decomposition process this will provide data on the extent of decomposition within a particle as a function of time and temperature. Thus, one would know the amount of porosity within the particle and the composition of the gases within the pores. This provides critical information for assessing the response of a damaged material after it is ignited or when it is subjected to a subsequent impact or shock. Since AP-based propellants typically have bimodal AP particle size distributions, these data can be obtained as a function of particle size so that the model of the propellant would be based on very realistic behavior of AP. For the dissociative sublimation process, our STMBMS data analysis process can be calibrated further than was done in the present experiments to provide accurate data on the gas-phase reaction processes. These data can then be combined with previous gas-phase results from the literature to provide an accurate assessment of the gas-phase reactions.

For the propellant, it is clear that we can obtain data on the reactions between AP and the binder and plasticizer. Since these constitute essentially all of the reactive ingredients in a thermal decomposition process, the STMBMS should be able to provide the data required to determine the reaction kinetics between the major ingredients in the propellant. In addition, it appears that the STMBMS can also be used to determine how fast the products, formed within a propellant sample, flow out of the sample. In the present experiments, we have observed significant changes in the rate of evolution of gas from AP, depending on whether or not it is in a propellant. We have also detected differences in the gas evolution rates that are dependent on the pressure of the gas that surrounds the propellant samples. These results indicate that it should be possible to characterize the flow rate of gases out of a propellant sample. For example, an experiment, in which propellant samples of different and well-characterized geometries are decomposed in the reaction cell, would provide data on both the chemical reaction kinetics of the AP,

the reaction of AP with the binder, and the flow rate of gas out of the propellant. In this way models of the main decomposition processes that occur within the propellant can be constructed and directly compared to the results of the STMBMS experiments.

CONCLUSIONS

The use of STMBMS for studying the decomposition of both pure AP and AP-based composite propellant provides detailed time-dependent quantitative data on the gas formation rates of the gaseous products formed in the decomposition of these materials. The results provide information on reactions that occur in both AP by itself and between AP decomposition products and the plasticizer and binder. This type of time-dependent gas-formation-rate data can be used to construct models of the thermal decomposition of AP-based composite propellants that will be useful in models of ignition and crucial for models of "slow-cookoff" events.

The decomposition of pure AP occurs in two distinct reaction processes. The first is a lower temperature decomposition that occurs in the solid phase and accounts for 25% of the decomposition with 200μ diameter particles and 13% decomposition with 20μ diameter particles. The second is dissociative sublimation of AP to NH_3 and $HClO_4$, followed by gas-phase reactions of these two sublimation products. The relative amounts of the various gas-phase decomposition products are determined by the extent of confinement of the products in the reaction cell.

The lower temperature process has been shown to be controlled by decomposition of AP within the solid particles. Our results for this lower temperature channel are not consistent with a surface reaction mechanism as proposed by Jacobs in the unified reaction model for AP decomposition. Some of the results of past experiments that were used to justify the surface reaction model, such as the presence of $HClO_4$ on the surfaces of decomposed AP and the fact that ammonia inhibits the lower temperature decomposition process are consistent with the observations of our experiments. In our experiments, we observe the evolution of $HClO_4$ to be delayed after the evolution of the more volatile products. Our interpretation of the results is that bubbles of decomposition products form within the AP particles and the surface at the bubble/solid AP interface is coated with $HClO_4$. When the bubble in the AP particle breaks, the volatile gases are vented and the $HClO_4$ adsorbed on the surface takes several minutes to evolve in our experiments.

In the AP-based composite propellant, AP decomposition follows the same two basic processes observed in the decomposition of pure AP. However, in the propellant the AP decomposition products react with the plasticizer and binder. In this process, products such as Cl_2 and O_2 from the lower temperature AP decomposition channel react with the plasticizer (if it hasn't already evaporated) to form HCl, H_2O and CO/CO_2 and with the binder to remove hydrogen from the polybutadiene. $HClO_4$, formed by the dissociative sublimation of AP, reacts with the binder to initially remove hydrogen, forming a carbonaceous residue. After most of the hydrogen is removed from the residue, $HClO_4$ resumes its gas-phase decomposition forming oxidative-type products, which react rapidly to form CO and CO_2 from the carbonaceous residue. If AP remains after the carbonaceous residue has reacted, reaction products similar to those observed in dissociative sublimation process of pure AP are observed.

ACKNOWLEDGMENTS

The authors thank Mr. D.M. Puckett for collecting the mass spectrometry data and to Ms. L. Dimeranon for supplying the AP and propellant samples. Work is supported by a Memorandum on Understanding between the DoD Office of Munitions and the Department of Energy under Contract DE-AC04-94AL85000.

REFERENCES

(1) Jacobs, P. W. M.; Whitehead, H. M. *Chemical Reviews* , **1969**, *69*, 551-590.
(2) Kishore, K.; Gayathri, V. Chemistry of Ignition and Combustion of Ammonium_Percholrate-Based Propellants. In *Fundamentals of Solid-Propellant Combustion*; Kuo, K. K., Summerfield, M., Eds.; American Institute of Aeronautics and Astronautics, Inc.: New York, NY, 1984; Vol. 90; pp Chapter 2, 53-119.
(3) Ramohalli, K. Steady-State Burning of Composite Propellants under Zero Cross-Flow Situation. In *Fundamentals of Solid-Propellant Combustion*; Kuo, K. K., Summerfield, M., Eds.; American Institute of Aeronautics and Astronautics, Inc.: New York, NY, 1984; Vol. 90; pp Chapter 2, 409-477.
(4) Dodé, M. *C. R. Acad. Sci., Paris* , **1935**, *200*, 63-66.
(5) Dodé, M. *Bull. Soc. Chim. France* , **1938**, *5*, 170.
(6) Jacobs, P. W. M.; Russell-Jones, A. *AIAA J.* , **1967**, *5*.
(7) Bircumshaw, L. L.; Newman, B. H. *Proc. Royal Soc.* , **1954**, *A227*, 228-241.
(8) Bircumshaw, L. L.; Newman, B. H. *Proc. Royal Soc.* , **1954**, *A227*, 115-132.

(9) Heath, G. A.; Majer, J. R. *Trans Faraday Society* , **1964**, *60*, 1783-1791.
(10) Kraeutle, K. J. "Scanning Electron Microscopy of Pure Ammonium Perchlorate after Its Reaction in the Orthorhombic and Cubic Phases"; 7th JANNAF Combustion Meeting, 1970.
(11) Behrens, R., Jr. *Reveiw of Scientific Instruments* , **1986**, *58*, 451.
(12) Behrens, R., Jr. *International Journal of Chemical Kinetics* , **1990**, *22*, 135-157.
(13) Behrens, R., Jr. *International Journal of Chemical Kinetics* , **1990**, *22*, 159-173.
(14) Behrens, R., Jr.; Bulusu, S. *Journal of Physical Chemistry* , **1992**, *96*, 8877 - 8891.
(15) Bircumshaw, L. L.; Newman, B. H. "The Thermal Decomposition of Ammonium Perchlorate," Explosives Research and Development Establishment, Waltham Abbey, Essex, England, 1951.

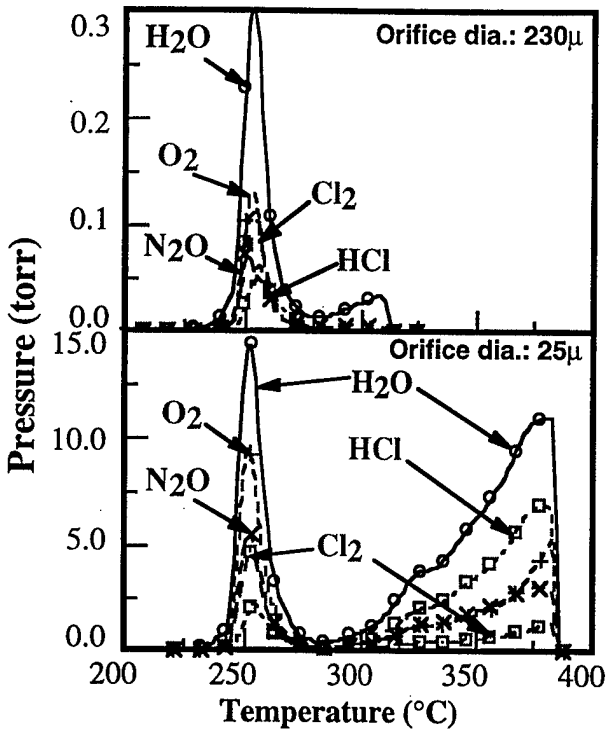

Figure 1. Pressure of reaction products in the reaction cell from thermal decomposition of 200μ diameter AP using 230μ and 25 diameter orifices on the reaction cell.

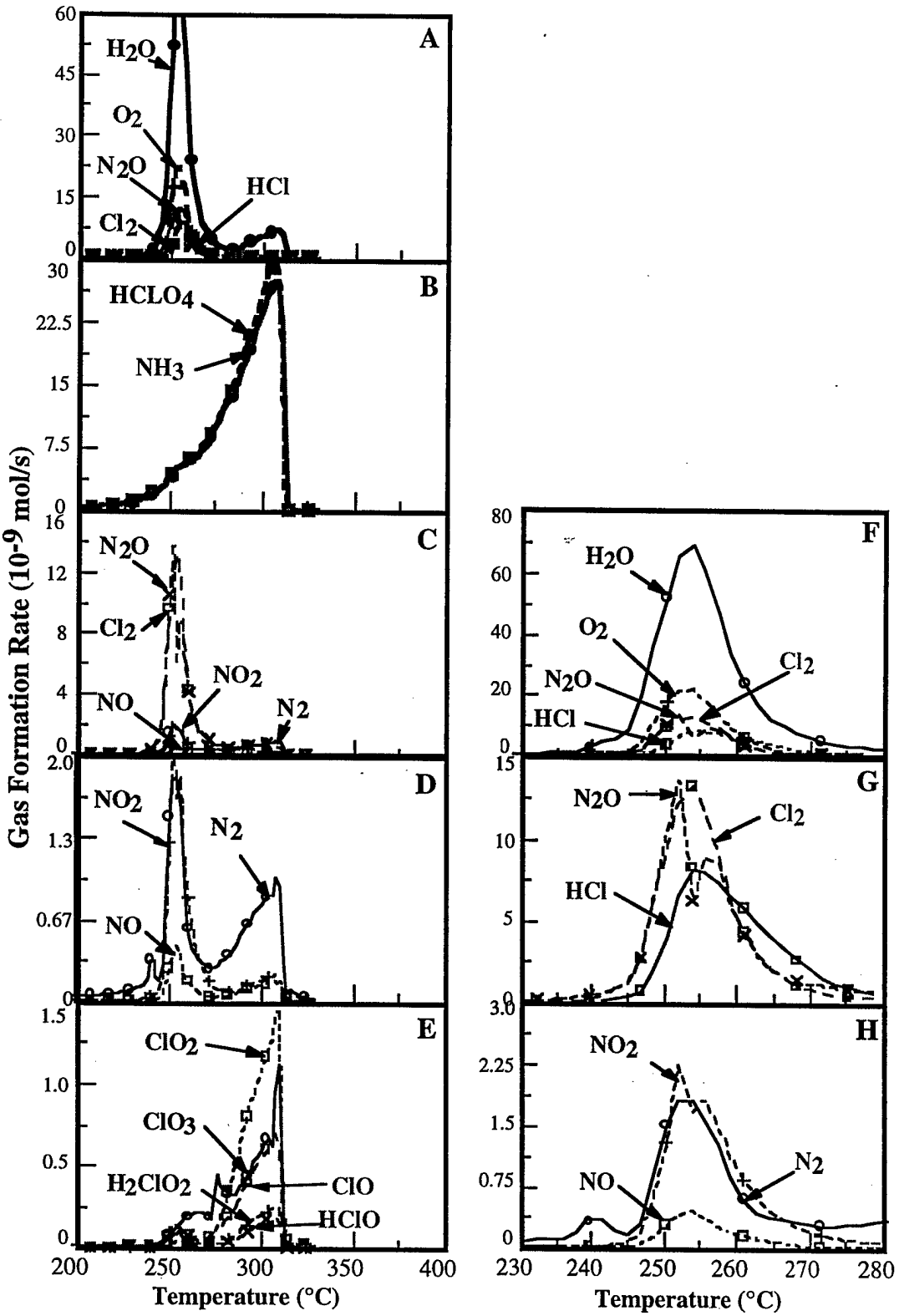

Figure 2. Gas formation rates of thermal decomposition products formed from the decomposition of AP in Experiment I. The AP particle diameter is 200μ, the reaction cell orifice diameter is 230μ, the heating rate is 1°C/min. The column on the right shows the products that evolve during the solid-phase decomposition. The fall in the N_2O signal at ~255°C is from noise in the data.

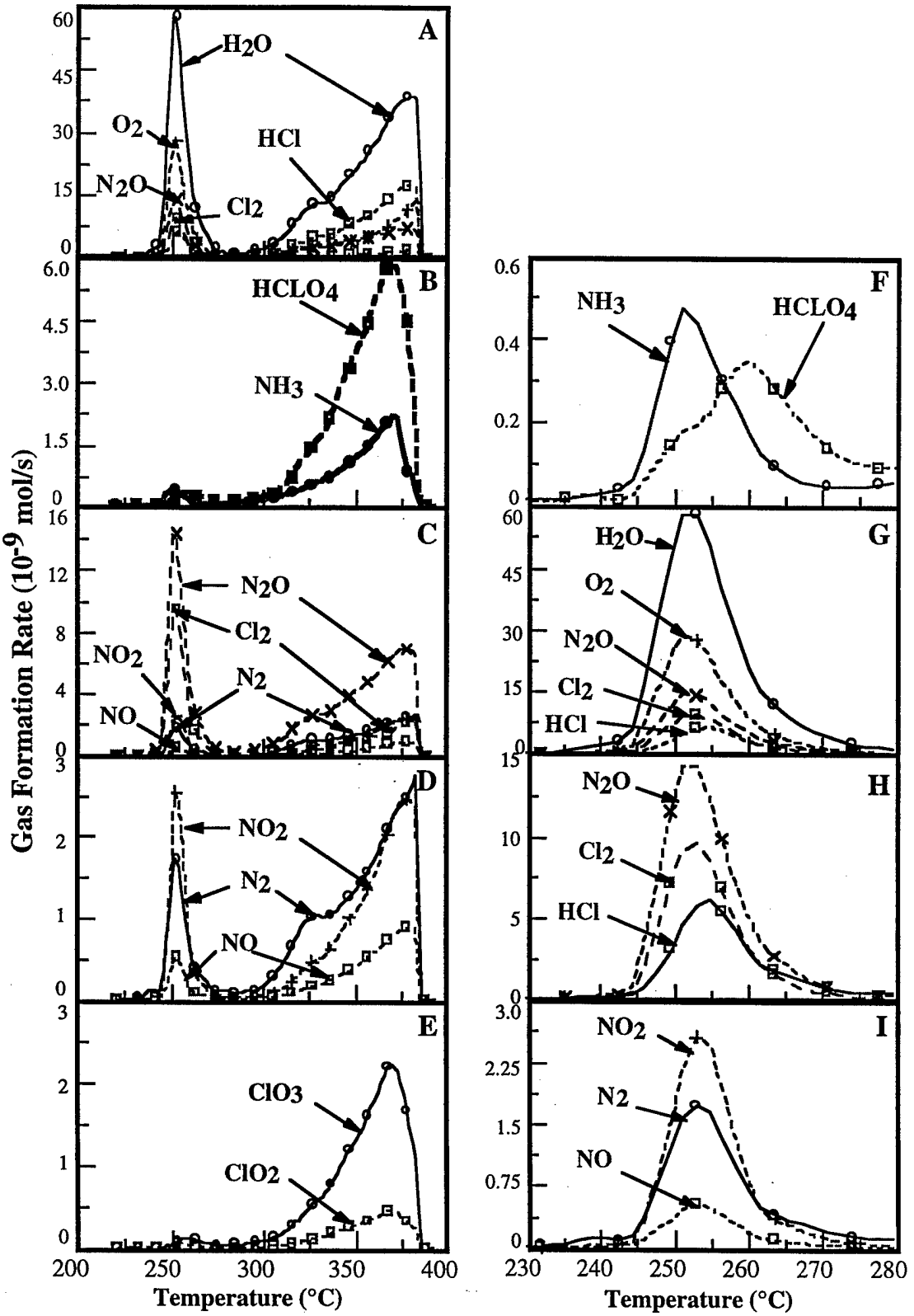

Figure 3. Gas formation rates of thermal decomposition products formed from the decomposition of AP in Experiment II. The AP particle diameter is 200μ, the reaction cell orifice diameter is 25μ, the heating rate is 1°C/min. The column on the right shows the products that evolve during the solid-phase decomposition.

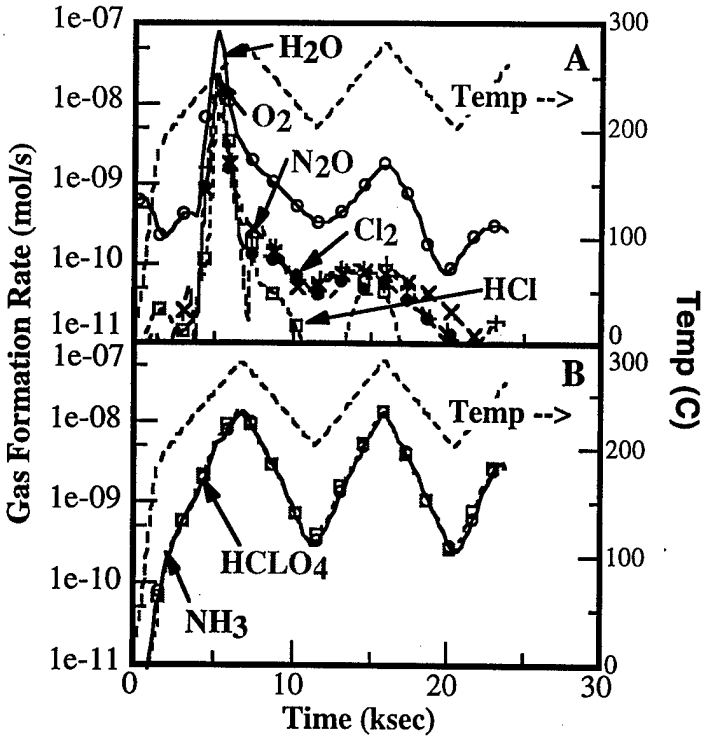

Figure 4. Gas formation rates of thermal decomposition products forme from the decomposition of AP in Experiment IV. The AP particle diam is 200μ, the reaction cell orifice diameter is 230μ, the heating rate is 1°C/min above 180°C and the temperature cycles between 200°C and 280°C. Note the lack of decomposition products, other than NH_3 and $HClO_4$ after the first cycle.

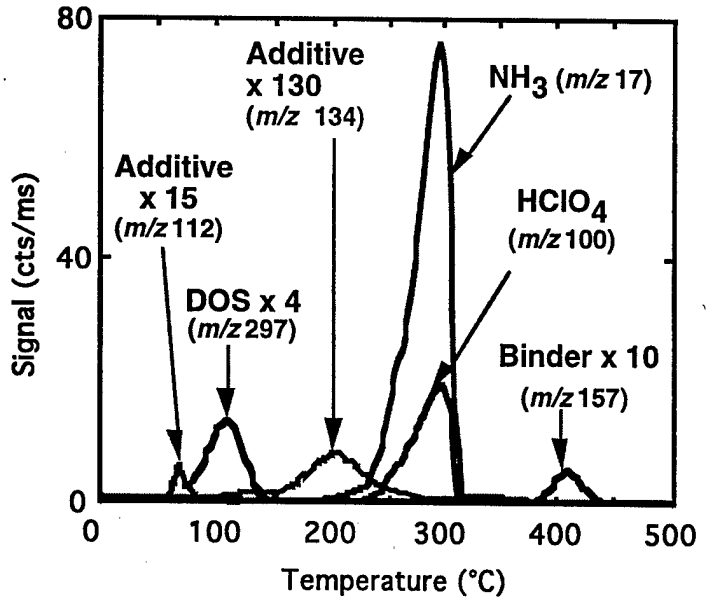

Figure 6. Separation of the plasticizer (DOS), AP (NH_3 and $HClO_4$), binder (*m/z*=157) and two additives (*m/z*=112 and 134) is acheived as an [AP/Al/HTPB] composite propellant is slowly heated at 1°C/minute in a reaction cell with a 230μ-diameter orifice.

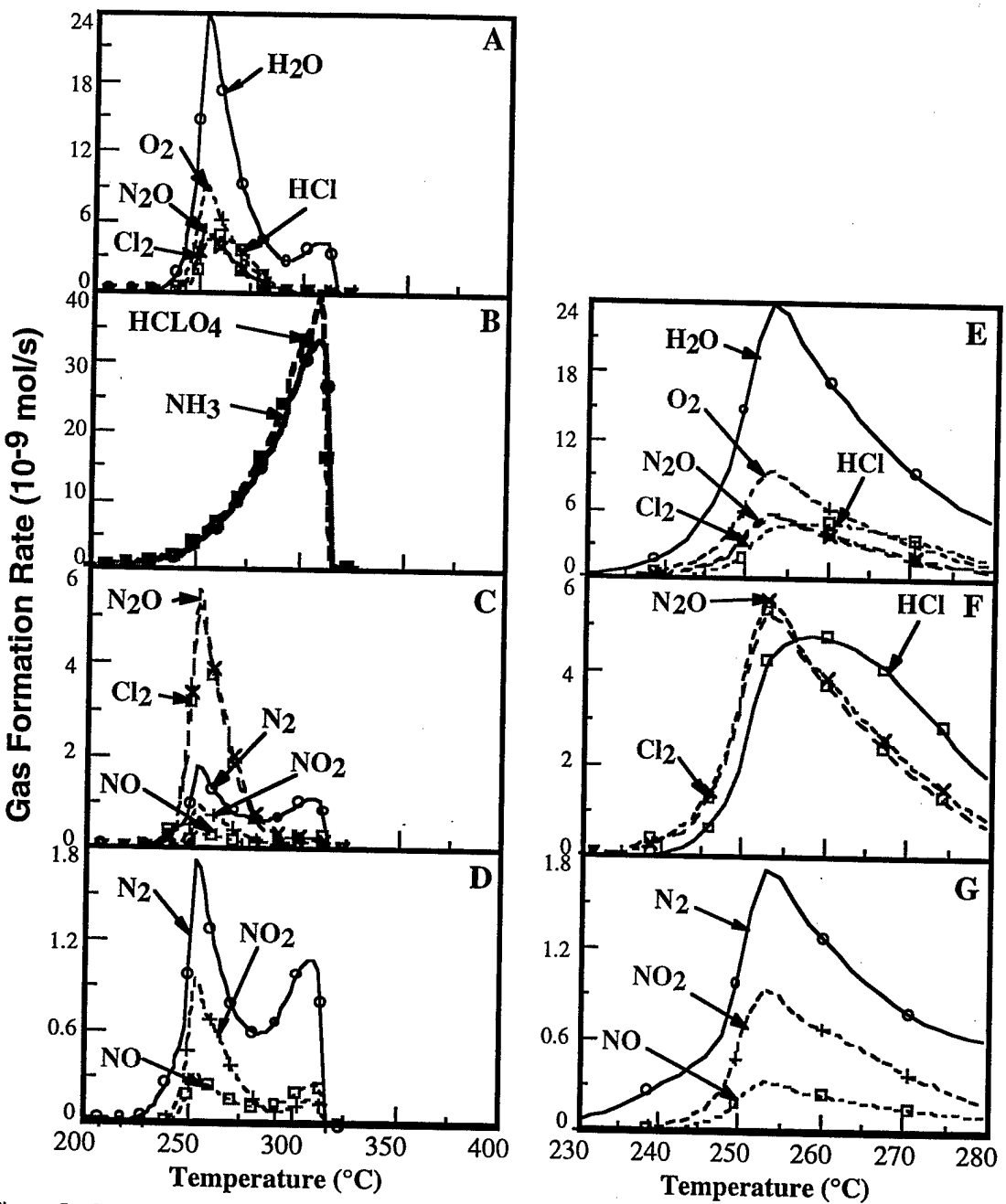

Figure 5. Gas formation rates of thermal decomposition products formed from the decomposition of AP in Experiment III. The AP particle diameter is 20μ, the reaction cell orifice diameter is 230μ, the heating rate is 1°C/min. The column on the right shows the products that evolve during the solid-phase decomposition.

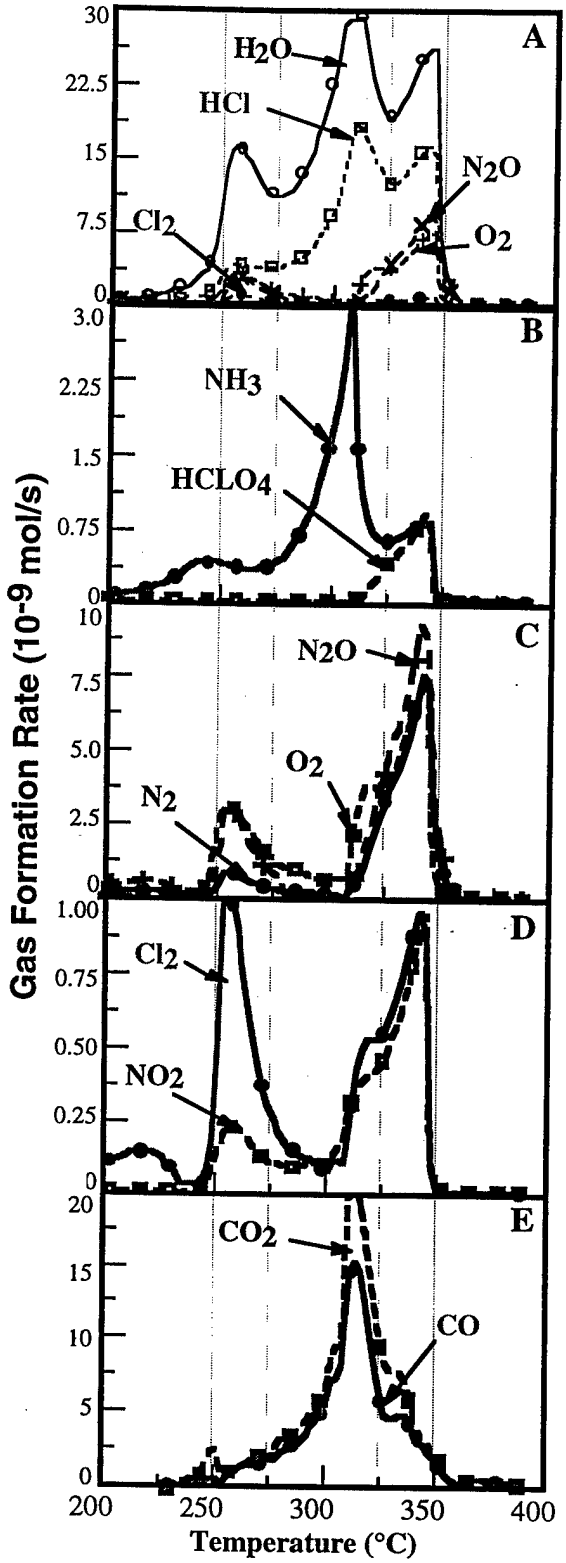

Figure 7. Gas formation rates of thermal decomposition products formed from the decomposition of the AP-based composite propellant in Experiment V. The reaction cell orifice diameter is 25μ, the heating rate is 1°C/min.

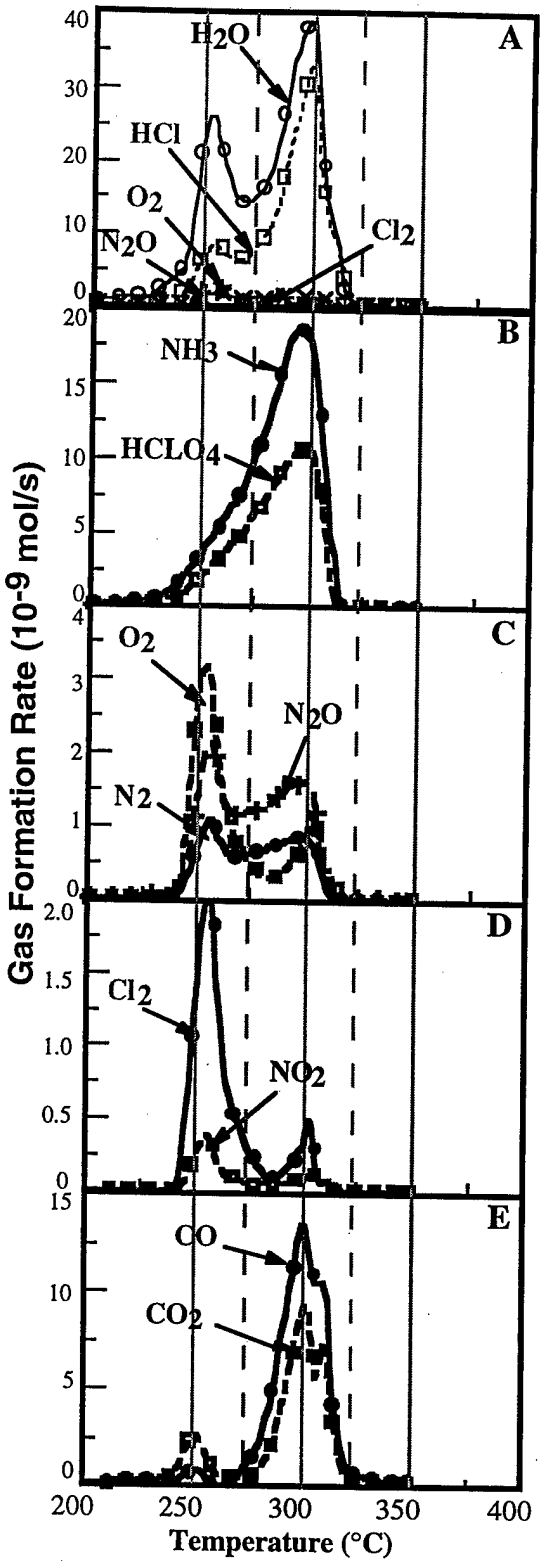

Figure 8. Gas formation rates of thermal decomposition products formed from the decomposition of the AP-based comoposite propellant in Experiment VI. The reaction cell orifice diameter is 230μ, the heating rate is 1°C/min.

Report Number (14) SAND--97-8422C
CONF-961194--

Publ. Date (11) 19980324
Sponsor Code (18) DOE/DP, XF
JC Category (19) UC-704, DOE/ER

DOE